

Thrust Performance Improvement of a Linear Induction Motor

Hyung-Woo Lee[†], Chan-Bae Park* and Byung-Song Lee*

Abstract – The end effect of a linear induction motor (LIM) has been known for several decades, especially in high speed operation. The exit part of the primary is not dealt as extensively as the entry part because of its minor effect. However, the exit part is one of the keys to weaken the dolphin effect, which occurs in high speed operation. In this paper, the concept of the virtual primary core is introduced, and chamfering of the primary outlet teeth is proposed to minimize the longitudinal end effect at the exit zone. For this, LIM for the high-speed train is designed and analyzed by using finite element method. Results confirm that chamfering can improve thrust performance effectively.

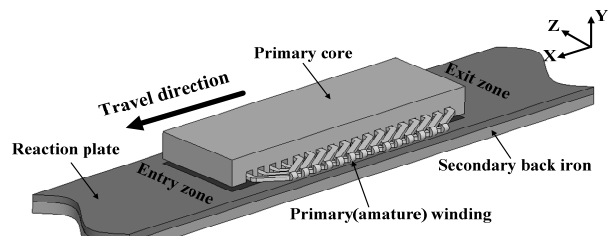
Keywords: End effect, Dolphin effect, LIM, Linear motor, Virtual primary core

1. Introduction

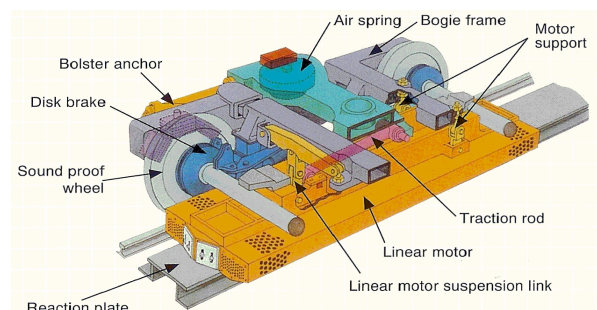
A linear induction motor (LIM) is a conventional rotary motor whose stator, rotor, and windings have been cut open, flattened, and placed on the guide way [1]. Fig. 1 represents the configuration of an SSSP (Single-Sided Short Primary)-type LIM and a practical application for railway. The primary is installed on the bogie under the vehicle and moves against the secondary, which is installed between rails on the ground. Although the operating principle is exactly the same as that of a rotary induction motor, the linear induction motor has a finite length of a primary or secondary parts causing a “longitudinal end effect” and a “transverse edge effect.”

Among the various LIMs, the SSSP is generally used for railway system because of the cheap construction cost. This SSSP-type LIM has numerous of advantages, including (1) excellent Accel. and Decel., (2) lower construction cost, (3) capability of climbing steep gradients, (4) ability to conduct flexible route planning by travelling through sharp curves, (5) less susceptibility to weather conditions, (6) quiet and smooth running operation (no mechanical couplings), and (7) less maintenance cost [2]-[5].

Yet, despite the advantages possessed by the non-adhesion propulsion system, LIM has low energy efficiency from the drag force and the leakage inductance resulting from the end effect and large airgap [1]. This chronic end effect is generated from the finite length of the primary part. Major longitudinal end effect is caused at the entry part of the LIM, and the minor end effect is caused at the exit part.



(a) Configuration of an SSSP-type LIM



(b) Practical application for a railway system [6]

Fig. 1. Linear induction motor and sample practical application.

2. End Effect of the High-speed Traction System

Fig. 2 shows the peak magnitude of the airgap magnetic flux density of the LIM in the longitudinal direction. The magnitude of the B_y at the entry and exit parts are different and are not uniformly distributed as the speed of the primary increases. Consequently, the primary experiences a different kind of normal force apart from the original normal force.

In other words, asymmetric airgap magnetic flux density at the end parts of a linear motor produces unbalanced normal force; as such, the airgap tends to increase at the entry and decrease at the exit part. This is called the “dolphin effect.”

[†] Corresponding Author: Department of Vehicle Dynamics & Propulsion System Research, Korea Railroad Research Institute, Korea. (krhwlee@krri.re.kr)

* Department of Vehicle Dynamics & Propulsion System Research, Korea Railroad Research Institute, Korea.

Received: May 14, 2010; Accepted: June 22, 2010

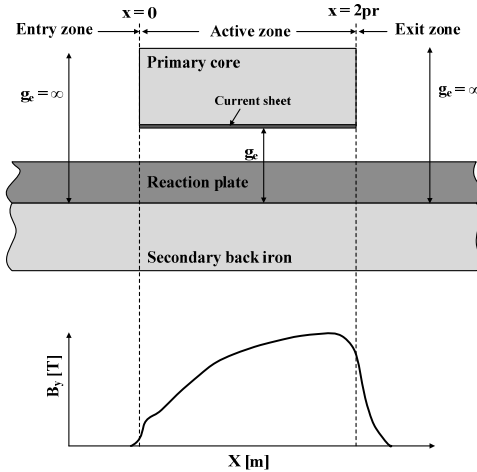


Fig. 2. Airgap magnetic flux density.

This airgap magnetic flux density of a LIM can be divided into the following:

$$B_y(x,t) = B_1(x,t) + B_{entry}(x,t) + B_{exit}(x,t), \quad (1)$$

$$B_1(x,t) = |B_s| \cos(wt - kx + \delta_s), \quad (2)$$

$$B_{entry}(x,t) = B_1 e^{-\frac{x}{\alpha_1}} \cos wt, \text{ and} \quad (3)$$

$$B_{exit}(x,t) = B_2 e^{-\frac{x}{\alpha_2}} \cos wt, \quad (4)$$

where B_s is the peak value of the wave travelling with synchronous velocity v_s , and B_1 and B_2 are the peak values of damped entry-end and exit-end waves travelling in the positive direction, respectively. In the above,

$$v_s = \frac{w}{k}, \quad k = \frac{\pi}{\tau} (\text{rad/m}).$$

From the unevenly distributed airgap magnetic flux density, the thrust force can be calculated as:

$$F_x = \frac{1}{2} \operatorname{Re} \left[\int_s J_e B_y^* ds \right], \quad (5)$$

where J_e is the induced current density, B_y is the y component of the airgap magnetic flux density, and d_s is the differential surface element.

Several researchers in the past have developed proper modeling techniques to analyze and explain the end effect, and some of these have proposed additional hardware to compensate for the flux at the entry part [7]-[16]. Although their proposed methods seem plausible, the installation of the additional part may be too difficult to practice. Therefore, although the end effect at the exit part is minor compared with the entry part, it cannot be ignored.

Given that additional hardware at the entry part cannot be installed in practice, the end effect at the exit part should be minimized by modifying the teeth shape in order to reduce the dolphin effect and improve the performance.

3. Proposed Design Methodology

Fig. 3 shows the airgap magnetic flux existing at the exit zone in the LIM. For a rotary induction motor, this flux does not exist inherently and every flux line makes an endless loop. Therefore, by introducing the concept of the virtual primary core, it can be assumed that a core similar to Fig. 4 [17] exists in the virtual core. The virtual primary core generates drag force and uneven normal force at the exit zone.

Accordingly, the exit end effect can be minimized by chamfering off the primary outlet teeth at the exit part and consequently removing the virtual core (Fig. 5). The angle α in Fig. 4 is 51° in the Mosebach model, but the angle will be changed depending on the airgap length and the tooth length of the analysis model.

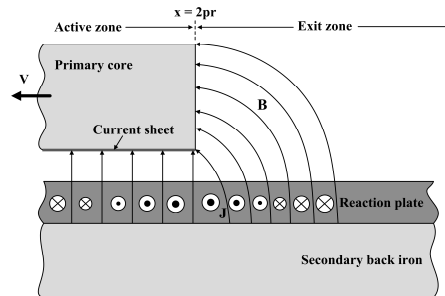


Fig. 3. Airgap magnetic flux at the exit zone.

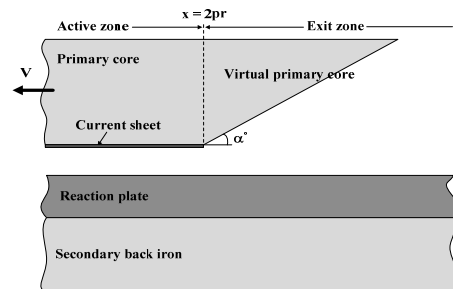


Fig. 4. Virtual primary core at the exit zone.

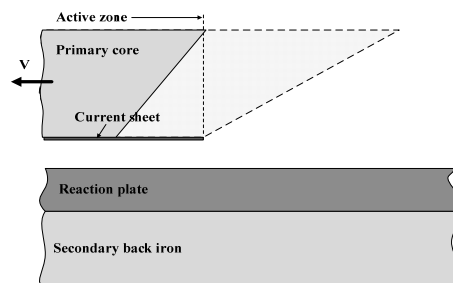


Fig. 5. Chamfering the primary teeth off at the exit zone.

4. Simulation

To verify the proposed methodology, an experiment must be conducted using an actual size motor. However, doing so may prove to be difficult due to the high costs of such an experiment. The LIM needs at least several tens of meters of long distance reaction plates along the track to reach the steady state and bogie with the wheels to attach the primary. Mobile measuring instruments should also be on board. Therefore, finite element analysis has been conducted in this research.

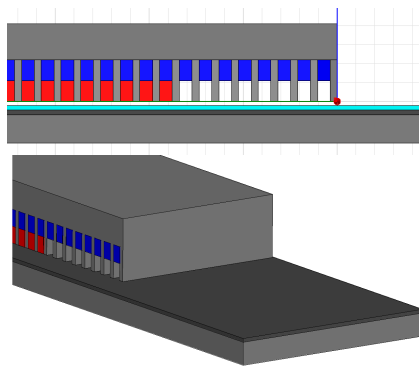
4.1 Analysis Model

Table 1 shows the main specifications of the LIM for the high-speed train. The rated output power was set to 100 kW and the power supply was DC 1,500 V. The LIM design was single-sided, short primary type, with 4 poles at the primary. The air-gap of the LIM was 9 mm and the pole pitch was 252 mm. The length of the LIM primary unit was 1,183.5 mm and the primary stack length was 230 mm. The double layer short-pitch winding and the 4 slots on each pole per phase resulted in the winding of the last 8 slots to become a single layer.

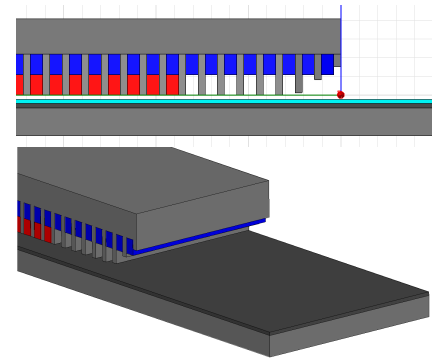
Given that the fringing flux at the exit part is nonlinear and varies with the geometric dimension and magnetic strength, the authors considered various cases of the chamfering angles ranging from 12.5° to 78°. Therefore, the outlet tooth of the primary core was divided into 4 equal parts of 11 mm in length, and the last 3 teeth were used for examination. Hence, the outlet tooth length changed from 11 to 33 mm based on the reference tooth length of 44 mm.

Table 1. Main specification of the LIM

Contents	Specification
Rated Output Power of LIM	100 kW
DC-link Voltage	1,500 V
Maximum Design Speed	165 km/h
Phase / Poles	3 ea / 4 ea
Air-gap / Al-Sheet Thickness	9 mm / 5 mm
Pole Pitch / Slot Pitch	252 mm / 21 mm
Number of slots per pole per phase	4 ea
Primary Stack Width	230 mm



(a) Reference model



(b) Proposed chamfered model

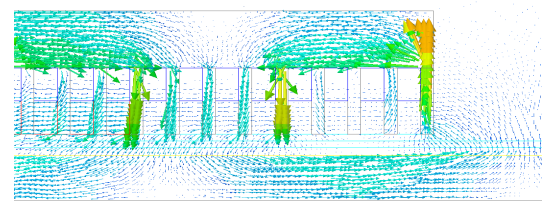
Fig. 6. Analysis models.

4.2 Analysis Results

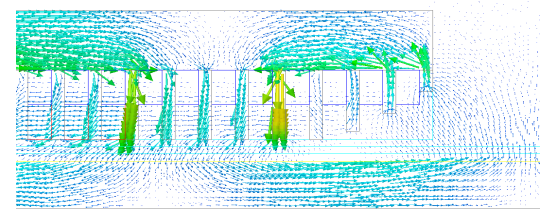
Fig. 7 shows the magnetic flux density vector distribution of the reference model and chamfered model at the exit zone. The velocity in the analysis is 165 km/h. For the reference model, the outlet tooth was saturated severely and the flux flowed outside from the last tooth as expected because of the longitudinal end effect. On the other hand, the magnetic flux of the chamfered model flowed almost evenly through the first, second, and third tooth from the outlet; the flux which flowed outside from the last tooth decreased. Therefore, severe flux saturation did not occur on the teeth, and the fringing flux also decreased.

Airgap flux density is represented in Fig. 8. The reference model had a relatively large amount of flux density, which resulted in the dolphin effect in a linear motor on the last tooth. However, the airgap flux density of the chamfered model has been diminished at the outlet. Consequently, normal force also decreased by about 5.12 % from 2,097.16 to 1,989.76 N.

Even with the decreased dolphin effect, thrust force should be maintained to satisfy the performance. Authors have analyzed several cases of varied chamfering models and obtained similar results (Fig. 9). Thrust force was almost



(a) Reference model



(b) Chamfered model

Fig. 7. Magnetic flux density vector distribution at the exit zone.

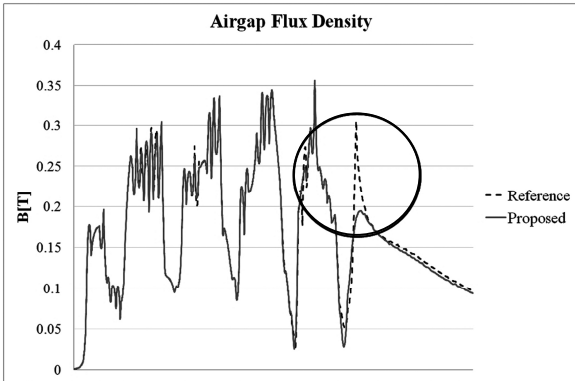


Fig. 8. Airgap flux density at the exit zone.

the same on both models, confirming that chamfering did not result in lost traction force. In addition, the thrust ripple decreased by about 4.5 %.

Results confirmed that chamfering effectively weakened the dolphin effect so as to decrease the thrust ripple with the same thrust force as the reference model.

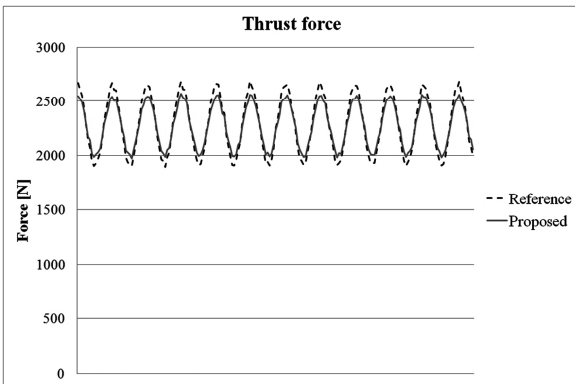


Fig. 9. Thrust forces of each model.

5. Conclusion

The exit end effect of a linear induction motor for the high-speed train propulsion system was considered in this paper. The exit end part created minor effect compared with the entry part, but it weakened the dolphin effect. Therefore, the concept of the virtual primary core was introduced and chamfering of the outlet teeth was proposed and simulated by using FEM. Results confirmed that chamfering was effective in reducing the thrust ripple without losing thrust force.

References

- [1] Hyung-Woo Lee, Ki-Chan Kim and Ju Lee, "Review of maglev train technologies," *IEEE Trans. Magnetics*, Vol. 42, No. 7, pp. 1917-1925, 2006.
- [2] Hyung-Woo Lee, Sung Gu Lee, Chanbae Park and Hyun-June Park, "Characteristic Analysis of a Linear Induction Motor for a Lightweight Train according to Various Secondary Schemes," *International Journal of Railway*, Vol. 1, No. 1, pp. 6-11, 2008.
- [3] Sakae Yamamura, "Theory of linear induction motors," *University of Tokyo Press*, 1978.
- [4] I. Boldea and S. A. Nasar, "Linear motion electromagnetic devices," *Taylor & Francis*, 2001.
- [5] Korea Railroad Research Institute, "Linear Electric Railway System," pp. 1-8, 2007.
- [6] Japan Subway Association, "Linear Metro System," pp. 1-28, 2004.
- [7] T. Hirasa, S. Ishikawa and T. Yamamuro, "Equivalent circuit of linear induction motors with end effect taken into account," *Electrical Engineering in Japan*, Vol. 100, No. 2, pp. 65-71, 1980.
- [8] J. F. Gieras, G. E. Dawson and A. R. Eastham, "A new longitudinal end effect factor for linear induction motors," *IEEE Trans. Energy Conversion*, Vol. EC-2, No. 1, pp. 152-159, 1987.
- [9] Y. Mori, S. Torii and D. Ebihara, "End effect analysis of LIM based on the wavelet transform technique," *IEEE Trans. Magnetics*, Vol. 35, No. 5, pp. 3739-3741, 1999.
- [10] N. Fujii and T. Harada, "A new viewpoint of end effect of linear induction motor from secondary side in ladder type model," *IEEE Trans. Magnetics*, Vol. 35, No. 5, pp. 4040-4042, 1999.
- [11] T. Higuchi, S. Nonaka and M. Ando, "On the design of high-efficiency linear induction motors for linear metro," *Electrical Engineering in Japan*, Vol. 137, No. 2, pp. 36-43, 2001.
- [12] N. Fujii, T. Harada, Y. Sakamoto and T. Kayasuga, "A compensation method for the end effect of a linear induction motor," *Electrical Engineering in Japan*, Vol. 143, No. 3, pp. 58-67, 2003.
- [13] N. Fujii, T. Kayasuga and T. Hoshi, "Simple end effect compensator for linear induction motor," *IEEE Trans. Magnetics*, Vol. 38, No. 5, pp. 3270-3272, 2002.
- [14] J. Jamali, "End effect in linear induction and rotating electrical machines," *IEEE Trans. Energy conversion*, Vol. 18, No. 3, pp. 440-447, 2003.
- [15] A. H. Selcuk and H. Koeroem, "Investigation of end effects in linear induction motors by using the finite-element method," *IEEE Trans. Magnetics*, Vol. 44, No. 7, pp. 1791-1795, 2008.
- [16] R. C. Creppe, J. A. C. Ulson and J. F. Rodrigues, "Influence of design parameters on linear induction motor end effect," *IEEE Trans. Energy conversion*, Vol. 23, No. 2, pp. 358-362, 2008.
- [17] H. Mosebach, "The effects of finite length and width in linear induction motors for both the short primary and the short secondary types," Ph.D dissertation (in German), *Technical University of Braunschweig*, Germany, 1972.
- [18] H. Lee, C. Park, B. Lee and H. Park, "Exit End Effect Reduction of a Linear Induction Motor for the Deep-underground GTX," will be presented in *ICEM*, 2010.



Hyung-Woo Lee received his B.S. and M.S. degrees in Electrical Engineering from Hanyang University in Seoul, Korea, in 1998 and 2000, respectively. He obtained his Ph.D. in Electrical Engineering from Texas A&M University, College Station, TX, in 2003. In

2004, he became a Post-doctoral Research Assistant at the Department of Theoretical and Applied Mechanics, Cornell University, Ithaca, NY. He served as a contract Professor at the BK Division of Hanyang University in Seoul, Korea in 2005. Since 2006, he has been a Senior Researcher at the Korea Railroad Research Institute in Uiwang, Korea. His research interests include design; analysis and control of motor/generator; power conversion systems; applications of motor drives, such as in Maglev trains, robots, and modern renewable energy systems.



Chan-Bae Park received his B.S. degree in Electrical Engineering from Chungnam National University in Taejon, Korea, in 2001. His M.S. degree in the same field was obtained from Seoul National University, Seoul, Korea, in 2003. He is currently enrolled in the Ph.D. program in Electrical Engineering at Hanyang University in Seoul, Korea. From 2003 to

2006, he worked as a Senior Engineer in Digital Appliance R&D Center at Samsung Electronics Co., where he developed various motors for home appliances. Since 2007, he has been a Senior Researcher at the Korea Railroad Research Institute in Uiwang, Korea. His research interests include design and analysis of motor/generator, transformer, and superconducting devices for energy conversion systems. Currently, he is developing a linear propulsion system for railway transits.



Byung-Song Lee received his B.S. degree in Electrical Engineering from Seoul National University of Technology, Seoul, Korea, in 1988. He obtained both his M.S. and Ph.D degrees in Electrical Engineering from Chung-Ang University, Seoul, Korea, in 1991 and 1995, respectively. From 1996 to

1997, he worked as Senior Researcher in Railway Vehicle R&D Center at KHRC (Korea High-Speed Rail Construction Authority), where he developed a propulsion system for high speed trains. Since 1998, he has been a Senior and Principal Researcher at the Korea Railroad Research Institute in Uiwang, Korea. His research interests include IPT (Inductive Power Transfer) and energy conversion systems for railway trains. Currently, he is working to develop an IPT system for railway vehicles.